RSC Advances

This article can be cited before page numbers have been issued, to do this please use: S. K. Chinnaiyan, M. Ayyavu, M. Gover Antoniraj, S. Vaidevi and K. Ruckmani, *RSC Adv.*, 2016, DOI: 10.1039/C6RA01482H.

ROYAL SOCIETY OF CHEMISTRY

www.rsc.org/advances

View Article Online
DOI: 10.1039/C6RA01482H

RSC Advances

ARTICLE

Ultrafast synthesis of stabilized gold nanoparticles using aqueous fruit extract of *Limonia acidissima L* and conjugated epirubicin: Targeted drug delivery for treatment of breast cancer

Received 00th January 20xx,
Accepted 00th January 20xx

DOI: 10.1039/x0xx00000x
www.rsc.org/

C.Senthil Kumar[a], Ayyavu Mahesh[c], M.Gover Antoniraj[a], S.Vaidevi[b] and K.Ruckmani[a,b,*]

In this study, the green chemistry approach was used for quick synthesis (within 30 seconds) of gold nanoparticles (AuNPs) by using the fruit extract of *Limonia acidissima L*. The study focused on the formation of *L. acidissima L* stabilized AuNPs without using any catalytic agent. The synthesis of the AuNPs was confirmed by observation of the surface plasmon resonance (SPR) band at 537 nm. On the surface of these capped AuNPs, epirubicin (EPI) was conjugated along with activated folic acid (FA) for targeted drug delivery. The EPI-FA-AuNPs complex was characterized using FTIR and UV-visible spectrophotometer and the AuNPs were characterized by HR-TEM, particle size analyzer, and zeta potential measurement. *In vitro* stability revealed that the AuNPs were stable in physiological conditions. The *in vitro* cytotoxicity of free EPI and EPI-FA-AuNPs was investigated against MCF-7 cells, and the results showed that 50% of EPI-FA-AuNPs was enough to achieve inhibition of growth (IC_{50}) and that the amount was lower than that of free EPI. Flow cytometry analysis showed significant reduction in G_2/M cells after treatment with EPI-FA-AuNPs, and molecular levels of apoptosis were studied using western blotting. Over all, the results revealed that the EPI-FA-AuNPs have better regression activity on tumor cells than free EPI.

1. Introduction

While chemotherapy drugs are effective, they, unfortunately, have a lot of side effects, namely: (i) the conventional cancer drugs are lethal and cause death of healthy cells as well as cancerous cells; (ii) the drugs have a short lifetime in the body and up to 90 % of intravenously delivered drugs may be gathered up by macrophages within the first 5 min of their entering the body; and (iii) the drugs have low solubility, and hence, it is necessary to deliver a larger dose of the conventional anticancer drugs in order to meet a good therapeutic index [1]. To overcome this problem, we have established a method to synthesize gold nanoparticles (AuNPs) functionalized with folic acid (FA) for targeted delivery of epirubicin (EPI), an anthracycline chemotherapy agent [2]. EPI has been clinically used to treat various types of cancer such as breast cancer, lymphomas, sarcomas in soft-tissue, pancreatic cancer, gastric cancer, small-cell lung cancer, and acute leukemia. EPI shows less hematologic or myocardial toxicity at comparable doses [3]. AuNPs are identified as favorable candidates for drug delivery applications due to their unique dimensions, tunable surface functionalities, nontoxicity, and controlled drug release capability [4]. Green chemistry-based eco-friendly methods are predominantly used for the synthesis of AuNPs instead of chemical synthesis [5]. Plant extracts are used as reducing and stabilizing agents to synthesise the nanoparticles. Plant extracts contain different concentrations and combinations of organic reducing agents, which influence the characteristics of the

a. *Department of Pharmaceutical Technology, Anna University BIT campus, Tiruchirappalli-620024, Tamilnadu, India. E-mail:rmani48@gmail.com, : Fax: +91-431-2407333: Tel* : +91-431-2459922.

b. National Facility for Drug Development for academia, Pharmaceutical and Allied Industries (NFDD), Anna University, BIT campus, Tiruchirappalli-620024, Tamilnadu, India.

c. School of Biological Sciences, Madurai Kamaraj University, Madurai 625021, India

View Article Online
DOI: 10.1039/C6RA01482H

nanoparticles produced [6]. Flavonoids, the plant metabolites, contain various functional groups capable of triggering nanoparticle formation. It has been suggested that the tautomeric transformation of flavonoids from the enol-form to the keto-form releases a reactive hydrogen atom that can reduce the metal ions into nanoparticles [7]. Fruits of *L. acidissima L*, contain higher quantities of flavonoids, tyramines, tannins, phytosterols, saponins, glycosides, carbohydrates, vitamins, coumarins, triterpenoids, and amino acids as their chemical constituents [8]. The targeted drug delivery system uses the anticancer drug for treatment of cancer cells alone, which reduces the effects of the drug on noncancerous cells and simultaneously increases its efficacy on cancer cells [9]. The main aim of using the targeted drug delivery system is to deliver the anticancer drug to the cancerous cells without loss of the drug's efficacy [10,11]. The folate receptor (FR) is a meticulously studied ligand for the selective delivery of anticancer drugs on FR-positive tumor cells [12]. In general, the FRs are highly up-regulated on the surface of different types of malignant cells [13]. In this study, the zebrafish embryo has been used as an *in vivo* prominent vertebrate model for assessing the toxicity of AuNPs. The zebrafish offers several advantages as a model for *in vivo* high-throughput drug screening. It is low cost, transparent, and the human genome and the zebrafish genome are highly comparable in terms of tissue types, fertilization, and the development of different systems and their active functions [14]. This article deals with the rapid green chemistry-based synthesis of AuNPs that can be used as a carrier for EPI, a drug used to treat breast cancer. Zebrafish embryos were used to examine the developmental toxicity of both normal and drug coupled AuNPs. The efficacy of both EPI and EPI-FA-AuNPs were tested on the MCF-7 cell line (breast cancer).

2. Experimental methods

Material

L. acidissima L fruit was used for this study. EPI HCl was obtained from SRL Limited, Mumbai (India). Hydrochloroauric acid (HAuCl4), FA, 1-(3-dimethylaminopropyl)-3-ethylcarbodiimide hydrochloride (EDC), and 3-(4, 5-dimethylthiazolyl-2)-2, 5-diphenyltetrazolium bromide (MTT) were obtained from Sigma-Aldrich Chemicals (USA). MCF-7 cell lines were obtained from National Center for Cell Science (NCCS), Pune, (India). The antibody to actin, Bcl-2, caspases-3 and caspases-8, Fas, FasL, and FADD bax were purchased from Santa Cruz Biotechnology, CA, USA and Neo Markers, USA. Millipore milli Q water was used for all the experiments. All other chemicals and reagents were of analytical grade.

Activation and attachment of FA to AuNPs

Activation of FA has been reported earlier by Pandey and coworkers [15]. It was carried out by dissolving 0.25 g of FA in 20 mL of dimethyl sulfoxide (DMSO), and the mixture was then subjected to sonication for 45 minutes. The carboxylate group of FA was activated by the addition of 0.225 gm of n-hydroxy succinamide (NHS) and 0.125 gm of dicarboxy aminocarbodiimide (EDC). The reaction was allowed to take place in an inert environment created by argon gas at 28 ^{o}C for 12 hours (FA/NHS/EDC molar ratio 2: 2: 1). The resultant mixture was filtered through Whatman filter paper and was used for further characterization. Attachment of FA was carried out by adding 9 ml of AuNPs to 1 ml of activated FA. The solution was purged continuously for 4 hours under N_2 atmosphere and stirred constantly using a magnetic stirrer. After 4 h, both inlet and outlet valves were sealed, and the solution was allowed to rest for 24 h. After 24 h the compound was filtered using Whatman filter paper and stored at 20 ^{o}C. Free FA was removed using a 3000 KDa dialysis bag against phosphate buffered saline (pH 7.2). The post-dialyzed samples were centrifuged at 6000 RPM for 15 min at 20 ^{o}C. The pellet was redialyzed with deionized water for 24 h under constant stirring. The samples were subjected to UV-Vis spectroscopy at systematic intervals for examination.

Synthesis of AuNPs-FA-EPI complex

EPI was conjugated to the AuNPs-FA complex for the destruction of cancer cells. Equimolar concentrations of EPI (0.25mM) and AuNPs-FA (0.25mM) were subjected to reduction with trimethylamine, 0.5mM (TEA) using DMSO as a solvent. The molar ratio of AuNPs–FA/EPI/TEA was 1: 1: 2. The mixture was purged using argon gas with continuous stirring at 50 ^{o}C for 4 h. The resultant EPI-FA-AuNPs conjugate was refined using dialysis against nano-pure water for three days with a dialysis tube (MW cut-off of 3000 Da) to remove the excess amount of unbound EPI molecules and DMSO. The water was changed at 6-hour intervals. The entire compound was characterized using UV-Vis spectrophotometry and FTIR.

Characterization of AuNPs and EPI-FA-AuNPs

Preliminary characterization of AuNPs and EPI-FA-AuNPs was carried out by FTIR, XRD, HR-TEM, particle size and zeta potential analysis method. LC–MS analysis of the extract was also been carried out. The detailed procedures are given as supplementary information.

In vitro stability studies

1 ml of AuNPs was incubated with 0.5 ml each of 0.9 % NaCl saline and phosphate buffer saline (PBS, pH 1.2, 4.5, 6.8 and 7.4),

View Article Online
DOI: 10.1039/C6RA01482H

respectively, at 37 °C for 48 hours and were analyzed spectrophotometrically by measuring at 480 nm.

In vivo toxicity study of AuNPs in zebrafish embryos

Fertilized eggs of zebrafish were obtained from the natural mating of adult zebrafish, and embryos were collected within 2 hours of spawning. Six healthy embryos from fertilized eggs, approximately 2 hours post fertilization (hpf), were transferred to each well of a 24-well plate containing 1 mL of the E3 medium. The embryos were exposed to different concentrations of AuNPs for 4 days. Duplicates were maintained without the AuNPs as control. Toxicity was assessed by studying the hatching rate, percentage survival rate, and morphology changes in the embryos.

Loading efficiency

From the total concentration of EPI used for loading onto AuNPs, the unloaded drug was removed by separating the supernatant after centrifugation (Eppendorf centrifuge 5430R) at 15,000 × g for 15 min. Free EPI present in the supernatant was determined by UV-Vis spectrophotometry by measuring at 480 nm.

The percentage of drug loading efficiency was calculated using the following formula (1)

$$\text{Drug loading efficiency} = \frac{\text{Theoretical amount of drug loaded - Free drug}}{\text{Theoretical amount of drug loaded}} \text{ X } 100 \ldots\ldots\ldots\ldots (1)$$

In vitro drug release characteristics

EPI-conjugated AuNPs (equivalent to 1000 µg of EPI) were dialyzed against 100 ml of sodium phosphate buffer (pH 5.7 and 7.4), at 37 °C with continuous stirring at 100 rpm. One milliliter of the sample was withdrawn at specific time intervals and analyzed spectrophotometrically. The sink condition was maintained by replacing equal volumes of the buffer. The release studies were performed in triplicate, and the average was taken. The percentage of drug release was calculated by the using following formula (2):

$$\text{Release (\%)} = \frac{\text{Released EPI}}{\text{Total EPI}} \times 100 \ldots\ldots\ldots\ldots\ldots\ldots (2)$$

In vitro cytotoxicity studies

Cell viability was measured by MTT assay described by Mossman and coworkers [16]. The detailed procedure is given as Supplementary information.

Apoptosis study

The influence of EPI-FA-AuNPs inducing apoptosis in the breast cancer cells was confirmed using staining methodology[17]. The detailed methodology is given as Supplementary information.

Flow cytometric analysis and Western blotting

To investigate the effect of the drug on the cell cycle distribution analysis described by Krishnan [18], Western blotting was carried out as described in another paper [19]. The detailed methodology descriptions are given in the Supplementary information.

High content imaging

Localization of EPI-FA-AuNPs and the cytotoxic effect were tested on MCF-7 cell line. Briefly, 2×104 cells/well of MCF-7 cancer cell line were seeded on 96 well CellCarrier microplates (PerkinElmer, US).When the cells reached 80% confluence, the medium was changed, and then the cells were treated with AuNPs, EPI, and EPI-FA-AuNPs, and the plate was incubated for 24 hours in a humidified incubator at 37 °C with 5% CO_2. The cells were washed twice with ice-cooled PBS, and the drug was localized in live cells using the Operetta High Content Imaging System (PerkinElmer, US).

3. Results and discussion

Characterization of EPI-FA-AuNPs

In the present study, we explain the reducing, stabilizing, and biocompatible properties of *L. acidissima L* extract for synthesis of AuNPs. *L.acidissima L* has higher quantity of polyphenolic compounds that can actively chelate and reduce metal ions to nanoparticles. It was assumed that the tautomeric conversions of flavonoids from the enol-form to the keto-form may release an

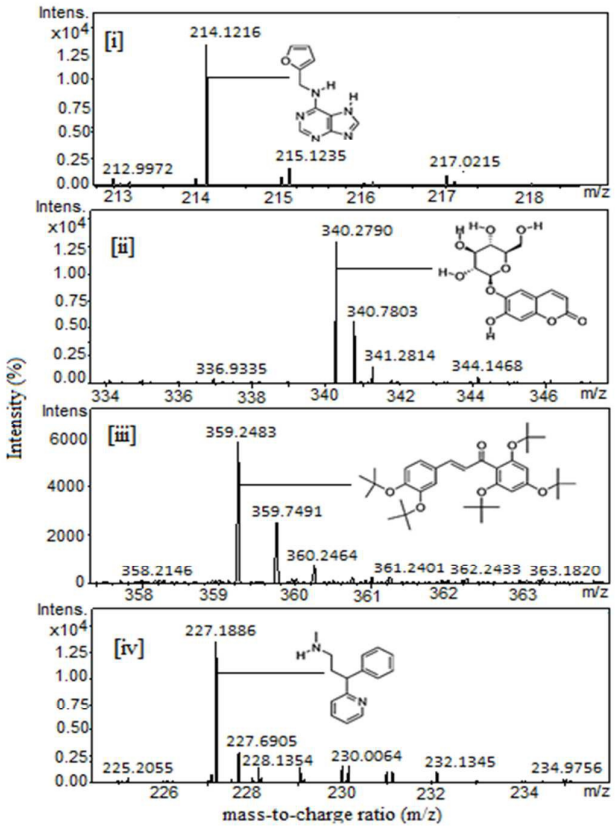

Fig. 1 . LC–ESI–MS/MS analysis of an optimised aqous extract of *Limonia acidissima L* fruit.

View Article Online
DOI: 10.1039/C6RA01482H

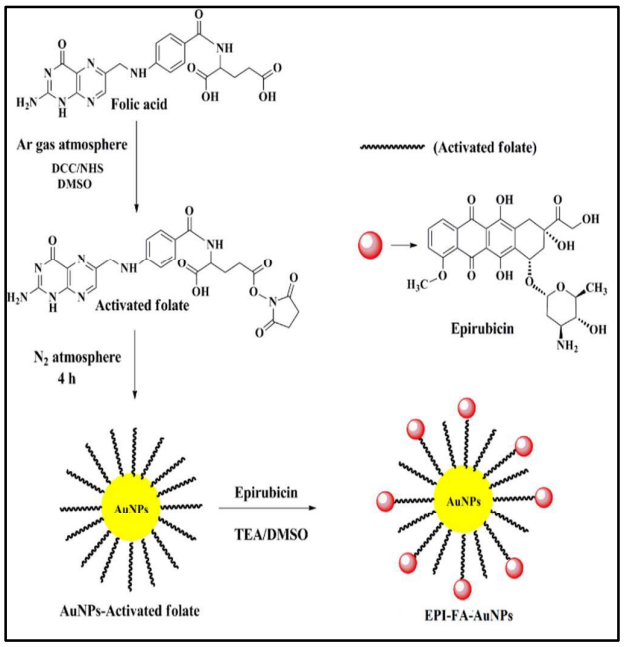

Scheme 1: Schematic representation for the generation of EPI-FA-AuNPs

activated hydrogen atom that can reduce metal ions to form nanoparticles (yellow color converted to wine red color).

The Photochemical profiling of the extract was done by LC-MS analysis which revealed the presence of phytocompounds such as (i) kinetin, (ii) esculin, (iii) 3,4,2',4',6'-pentamethoxychalcone, (iv) N-desmethylpheniramine. The identification of compounds was verified by mass fragmentation analysis, and the LC-MS spectra of the compounds are shown in Figure 1. The combined action of these chemical components and others may be responsible for the observed reduction of the metal ions to form nanoparticles. The AuNPs were formed by simple mixing without applying any external energy (heating, sun light, or microwaving). The resultant mixture produced a significant color change (to wine red) within a few seconds after the addition. Further, our study focused on using the synthesized AuNPs to enable conjugation of biomolecules for different applications in drug delivery **(Scheme 1)**.

We observed that the solution containing gold ions (Au^{3+}) and *L. acidissima L* turned into wine red (537 nm) within 30 seconds (The synthesis of AuNPs is given in the video file).We found that 75µL of *L. acidissima L* extract Figure 2 A was sufficient to reduce 1mM $HAuCl_4$. FTIR spectrum of *L. acidissima L* extract Figure 1B (i)) shows apeak at 3448 cm^{-1}, which could be attributed to the phenolic hydroxyls (O-H bond) in extracts, the absorption peaks at 1048 and 1612 cm^{-1} representing costretching functional present in the extract. Further, carboxyl stretching vibration peak formed at 1730 cm−1

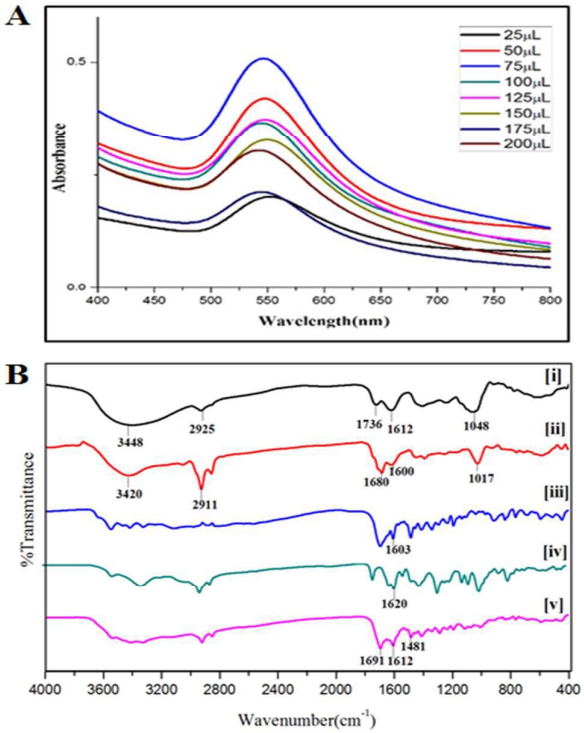

Figure 2: (A) Optimization of AuNPs by changing various concentrations of (*L. acidissima L* extract) while keeping the gold solution constant. (B) FT-IR study of: (i) *L. acidissima L* extract (ii) AuNPs (iii) FA (iv) EPI (v) EPI-FA-AuNPs.

However, in the FTIR spectrum of AuNPs Figure 2 B (ii), the peak at 3420 cm^{-1} becomes comparatively narrow, which could be attributed to the phenolic hydroxyls (O-H bond) confirming that the phenolic hydroxyls react with the AuNPs resulting in the partial destruction of the hydrogen bonds in the molecules of the *L. acidissima L* extract. A shift in the peak from 1048 cm^{-1} to 1017 cm^{-1} also indicates that *L. acidissima L* extract interacts with AuNPs through its adjacent phenolic hydroxyls and/or formed quinones. The comparison of FTIR spectra of bare AuNPs, FA, EPI, and EPI-FA-AuNPs shows that the spectrum of FA-AuNPs exhibits the characteristic IR absorption peaks of FA Figure 2B (iii), showing a peak at 1697cm^{-1} (amide I stretching), 1603 cm^{-1} (amide II stretching), and 1481cm^{-1} (hetero-ring, conjugated double bond). FTIR spectra of EPI and EPI-FA-AuNPs are shown in Figure 2B (iv) and (v). FTIR spectra of EPI clearly confirm the basic structural units such as OH, CH, and carbonyl groups carboxyl groups by the peaks that appear at 3300 cm^{-1}, 2940 cm^{-1}, and 1620 cm^{-1}, respectively. The FTIR spectrum of EPI-FA-AuNPs shows the peaks at 3300 cm^{-1} and 2940 cm^{-1}, demonstrating the OH and CH content of EPI-FA-AuNPs. Moreover, the disappearance of the peak at 1730 cm^{-1} describes the amide bond formation between the carboxyl functional of EPI and amine functional of FA. These spectra

View Article Online
DOI: 10.1039/C6RA01482H

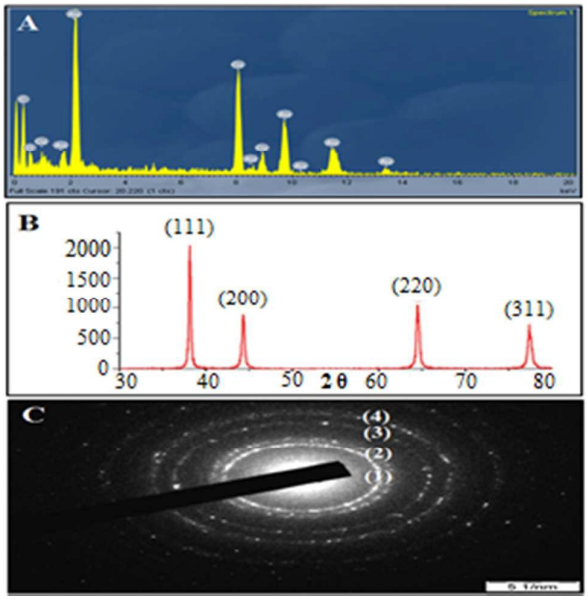

Figure 3: (A) The EDAX spectrum, (B) X-ray diffraction (XRD) spectrum, (C) SAED pattern of *L. acidissima L* fruit extract reduced AuNPs.

confirm the formation of EPI-FA-AuNPs. Energy dispersive X-ray (EDX) spectrum analysis of AuNPs showed the presence of AuNPs in the sample. In Figure 3 (A) reveals a strong and typical optical absorption peak at approximately 2.2 keV, which could be attributed to the SPR of the metallic Au nanocrystals. The crystalline structure of nanoparticles was determined based on X-ray diffraction (XRD) analysis. The crystalline peaks that were identified as AuNPs based on XRD analysis showed that the intense peaks of reflected radiation (Bragg peaks) were at the points (1 1 1), (2 0 0), (2 2 0), and (3 1 1) and were the diffraction lines of the face-centered-cubic (fcc) gold are shown in Figure 3 (B). The selected area of electron diffraction (SAED) outline of the AuNPs showing that the rings designated 1, 2, 3, and 4 arise because of the reflections from (1 1 1), (2 0 0), (2 2 0), and (3 1 1) are shown in Figure 3 (C). The morphological results (HRTEM) images Figure 4 (A) reveals that the AuNPs and EPI-FA-AuNPs appear to be nearly spherical in shape as seen in Figure 4 (B). The stability of EPI-FA-AuNPs in different buffers was examined in Figure 4 (C), and only slight changes (< 15%) were observed in the SPR band at 537 nm when the AuNPs were exposed to different buffers for 48 hours. However, at pH 1.2, about 20% decline in the absorbance at 537 nm was observed compared with the absorbance of EPI-FA-AuNPs at pH (7.4). The observed reduction in the absorption of EPI-FA-AuNPs in extremely acidic conditions could be attributed to the limited aggregation of EPI-FA-AuNPs as a result of the screening of the negative charge on the external of the AuNPs at pH (1.2). The results from these *in vitro* stability studies established that the AuNPs were intact and

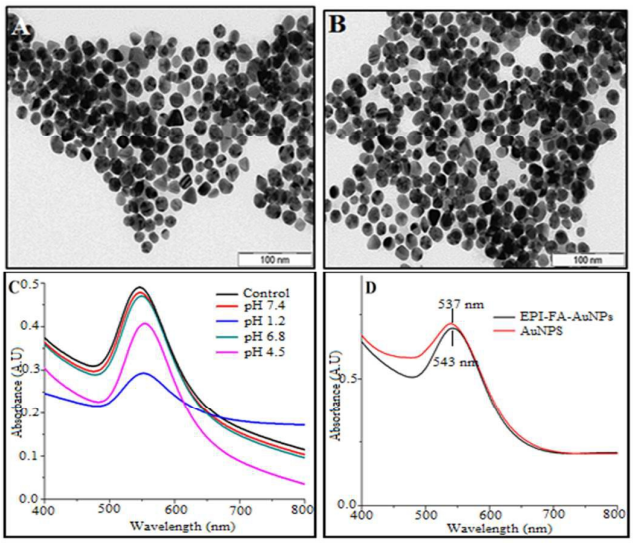

Figure 4: HRTEM image of (A) AuNPs (B) EPI-FA-AuNPs, (C)The UV–Vis spectra showing the *in vitro* stability of EPI-FA-AuNPs in the pH range 1.2–7.4 and PBS, (D) AuNPs conjugated EPI-FA-AuNPs.

demonstrated excellent *in vitro* stability in biological fluids at various pH [20]. EPI binding onto the AuNPs was further confirmed by the shift of the SPR band in Figure 4 (D) towards a higher wavelength (from 537 nm to 543nm). The percentage of EPI loaded onto the AuNPs was determined based on EPI content in the obtained pellet, and it was found that 52 ± 4% of the drug could be loaded. Inductively coupled plasma optical emission spectrophotometer (ICP-OES) was performed to quantify the amount of gold in the aqueous solutions of AuNPs, and the same was used in further studies.

Particle size and zeta potential measurements

The hydrodynamic particle size of the AuNPs was found to be 134 ± 4 nm with a polydispersity index of 0.219 are shown in Figure 5 (i). The average hydrodynamic diameter of EPI-FA-AuNPs is 139 ± 3 nm with a polydispersity index of 0.249 shown in Figure 5 (ii). A low polydispersity index shows that the particle size distribution of the AuNPs and EPI-FA-AuNPs is uniform. Zeta potential is considered an essential parameter to study the surface charge of the nanoparticle surface and predict the long-term stability of the nanoparticles [21]. The zeta potential of the AuNPs was found to be −27.9 mV Figure 5 (iii) indicating that the AuNPs were properly capped with anionic (carboxyl group) FA. EPI-FA-AuNPs were isolated by centrifugation and then suspended in an aqueous solution to quantify the electrophoretic mobility. The calculated zeta potential of EPI-FA-AuNPs was −16.0 mV as seen in Figure 5 (iv). Though

View Article Online
DOI: 10.1039/C6RA01482H

the surface charge is reduced to some extent, EPI-FA-AuNPs has found to be stable without aggregation when analysed after six-month storage period. Hence, it is clear that EPI-FA-AuNPs are highly stable over a reasonable period of time.

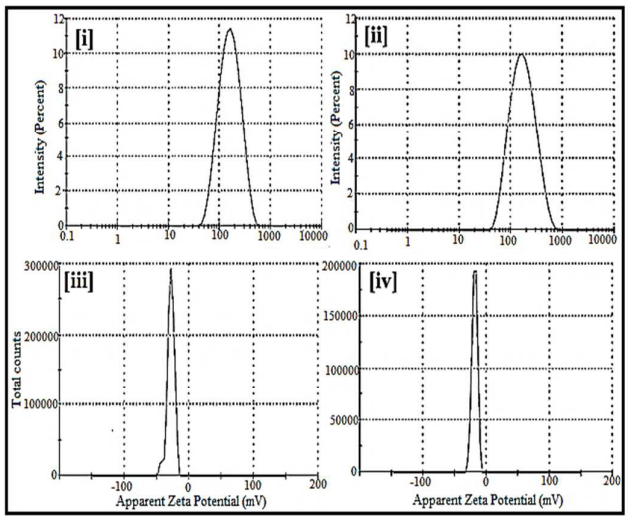

Figure 5: (i) The particle size distribution of AuNPs (ii) EPI-FA-AuNPs (iii) The zeta potential distribution of AuNPs in an aqueous medium. (iv)The zeta potential of distribution EPI-FA-AuNPs in an aqueous medium.

Toxicity of AuNPs in zebrafish embryos

Zebrafish embryos, which are ideal organisms, were used to investigate the developmental toxicity of AuNPs without EPI-FA [22]. The survival rate was better for the embryos that had hatched within 96 hours post fertilization, as compared with the control group as seen in Figure 6 A (i). The mortality level was indicated by the dead embryos 96 hours post fertilization as compared to the control group in Figure 6 A (ii).The survival rate and mortality rate examined shows no apparent toxicity at various concentrations ranging from 50 to 450 µg/mL [23]. The AuNPs-treated embryos were observed using a compound stereo microscope to find abnormalities such as pericardial edema, pigmentation, deformity of the pericardial sac of the larvae, and deformity of the tail. Exposure of zebrafish egg embryos to AuNPs did not produce any seeming toxicity in the development of the zebrafish are shown in Figure 6 A (iii). Hence, this investigation of results clearly indicated that the AuNPs might be carriers for drug delivery applications.

Release profile of EPI-FA-AuNPs

The *in vitro* study of pH-controlled EPI release from the EPI-FA-AuNPs was performed in PBS (pH = 7.4) and acetate buffer (pH = 5.7) at 37 ^{o}C, pH (7.4) and pH (5.7) being near the physiological and endosomal pH conditions, respectively, of a cancer cell. The results are presented in Figure 6 (B),The pH-dependent drug release is also considered to be an essential factor in cancer therapy [24]. The EPI-FA-AuNPs displays the slow and controlled release of the drug, with the release rate calculated showing negligible release when compared to that of free EPI in acidic and neutral atmospheres, respectively.

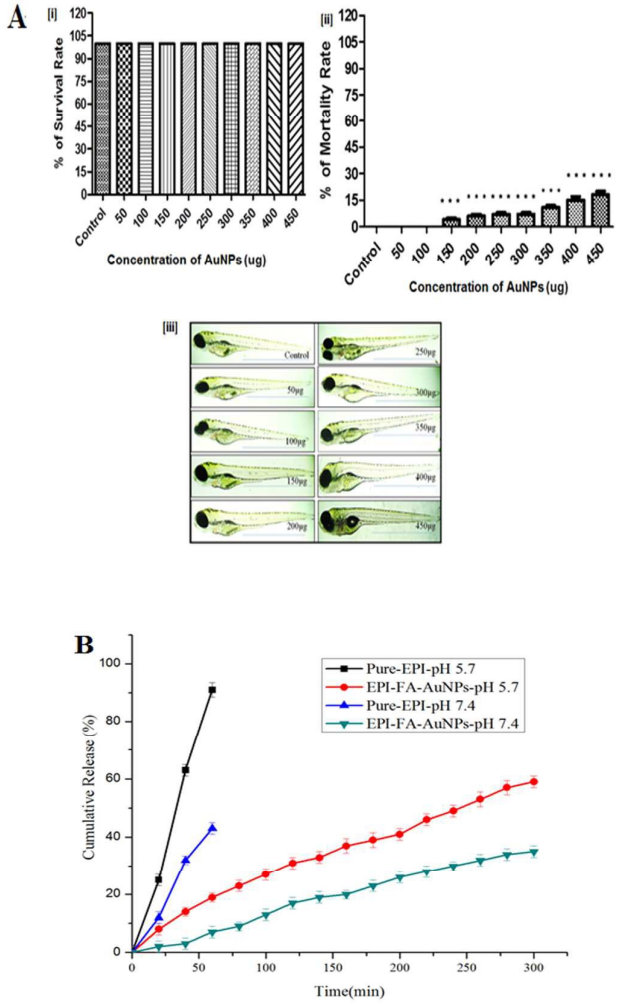

Figure 6: (A) (i) Graph representing the toxicity of AuNPs in terms of survival rate (%) of larvae, (ii) Mortality rate (%) analysis of AuNPs toxicity, (iii) Examples of zebrafish larvae exposed to control and various concentrations of AuNPs. Significant differences compared to control calculated with the one-way ANOVA test and are indicated by ***p < 0.001. (B) *In vitro* release profiles of EPI from the EPI-FA-AuNPs and free EPI in phosphate buffer solution (pH5.7 and 7.4) at 37 ^{o}C.

Furthermore, the release efficiency of the drug from the EPI-FA-AuNPs was rapid, higher at pH (5.7) than at pH (7.4) EPI from EPI-FA-AuNPs in pH (7.4) will help to reduce toxicity of EPI to the normal tissue since the physiological pH of the body is maintained at pH (7.4) [25].

In vitro cytotoxicity studies

To determine the cytotoxic effect of EPI and EPI-FA-AuNPs, cell viability study was done by a standard MTT-reduction assay with slight modifications [26]. The results of the MTT assay for free and EPI-

View Article Online
DOI: 10.1039/C6RA01482H

FA-AuNPs on MCF-7 cell lines are shown in Figure 7 (A). The IC_{50} value for EPI-FA-AuNPs was found to be around 2 µg/mL, while that

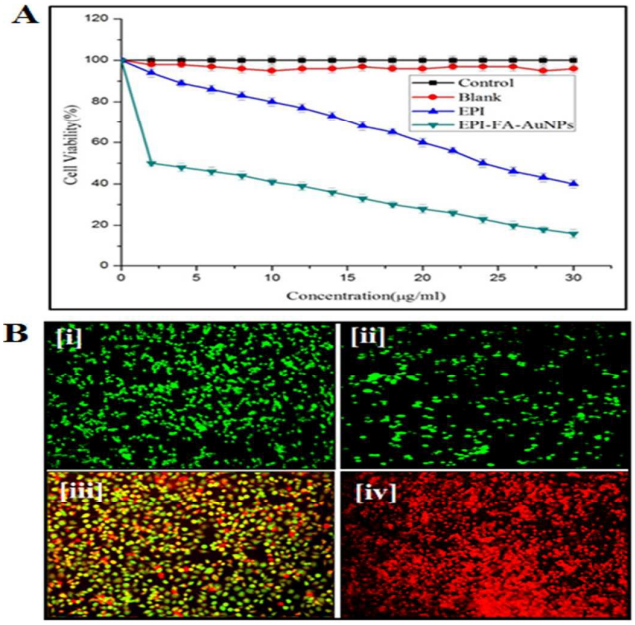

Figure 7: (A) *In vitro* cytotoxicity studies of drug EPI and EPI-FA-AuNPs in MCF-7 cell lines. All assays were performed in triplicate, and the mean ± standard deviations are shown. (B) Images of MCF-7 cell lines visualized under inverted microscope. (i) Control, (ii) Blank, (iii) EPI, and (iv) EPI-FA-AuNPs.

for free EPI ranged from 28 µg/mL on the MCF-7 cells. These results show that the EPI-FA-AuNPs exhibited better cytotoxic activity than free EPI. This could possibly be due to the result of the variations in the cellular uptake profile leading to better activity of EPI-FA-AuNPs as suggested by Ormrod and coworkers [27]. The results of this study suggests that FA functionalized AuNPs can effectively deliver the drug to MCF-7 cancer cells by means of active targeting.

Apoptosis study

Apoptotic changes, cytotoxic effect caused by EPI-FA-AuNPs occurred in MCF-7 cells when treated using acridine orange/ethidium bromide differential staining method. The stained cells characterized to EPI-FA-AuNPs caused more effective cell death than free EPI. The number of nonviable cells increased dramatically after treatment with EPI-FA-AuNPs in MCF-7 cells are shown in Figure 7 B (iv). The red color is due to the nonviable cells (dead cells), and it was revealed that EPI-FA-AuNPs treatment resulted in a significant increase in apoptosis compared to EPI treatment. The control and blank cells in Figure 7 B (i) and (ii), the condensed nuclei, as well as the membrane blebbing fluoresced uniformly bright green indicating (early apoptotic) that they did not undergo any apoptotic changes.

Effect of EPI-FA-AuNPs on cell cycle analysis

Generally, the flow cytometry study was performed to investigate whether apotosis and the cell cycle arrest are closely related. In our

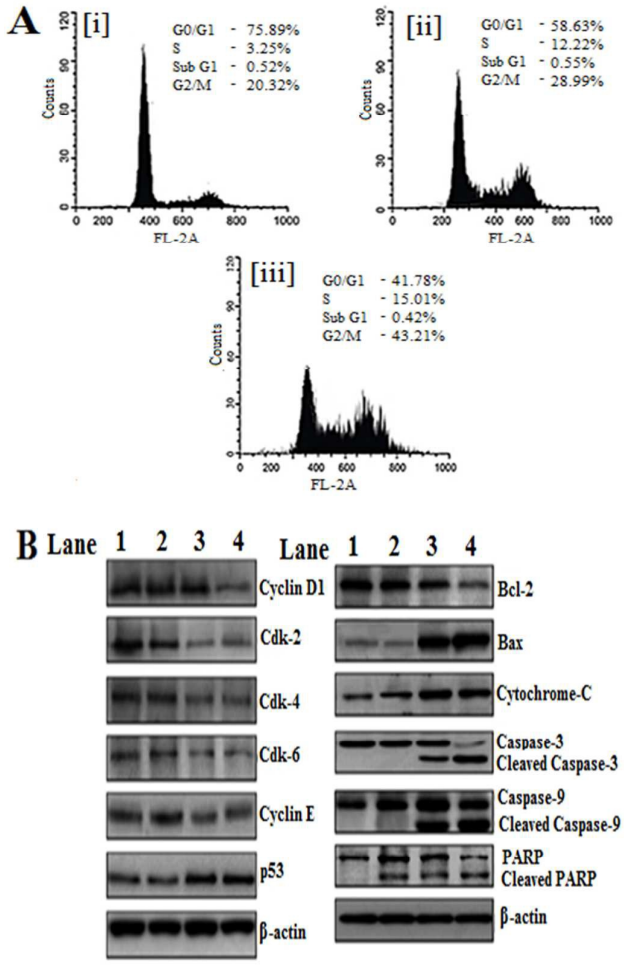

Figure 8: (A) Effects of EPI-FA-AuNPs on cell cycle analysis. MCF-7 non-small cell breast cancer cells were cultured for 36 hours (i) Control (ii) EPI (iii) EPI-FA-AuNPs. (B) Western blot, illustrating the different protein expressions in apoptosis after treatment with EPI and EPI-FA-AuNPs. Lane 1: Control, Lane 2: AuNPs, Lane 3: EPI, Lane 4: EPI-FA-AuNPs.

study, the effect of EPI and EPI-FA-AuNPs-on cell cycle (MCF-7 cells) was studied. Figure 8 (A) shows the cell cycle analysis of (i) control, (ii) EPI and (iii) EPI-FA-AuNPs. Control cells after 36 hours had 20.3 % the proportion of cells in the G_2/M phase in Figure 8 (A) (i), and the EPI and EPI-FA-AuNPs produced a dramatic increase of 28.95 % in Figure 8 (A) (ii) and 43.21% are shown in Figure 8 (A) (iii) in the G_2/M population, respectively. These data clearly prove that the cell cycle is arrested significantly at the G_2/M phase in EPI-FA-AuNPs induced MCF-7 cells [28]. The anti-cancer therapy completely eradicates the cancer cells by triggering different

View Article Online
DOI: 10.1039/C6RA01482H

caspase-mediated cell death pathways [29], which confirms the activation of the apoptotic pathway after EPI-FA-AuNPs' exposure.

Western blot analysis

The Western blot results showed mechanisms of EPI-FA-AuNPs-mediated cell death; the apoptotic regulators have been measured using mRNA and protein expression patterns. Cyclin D1 regulates the proliferation process by adjusting its expression levels and, accordingly, regulates the cell cycle control machinery [30]. EPI controls the reduction of Cyclin D1 levels in tumors [31]. The results as seen in Figure 8 (B) showed that EPI-FA-AuNPs inhibited the function of Cyclin D1, and its expression was dramatically diminished. Cyclin E showed a high intense band when AuNPs and native EPI-treated cells were compared. The functions of Cyclin-dependent kinase CDK4, CDK6, and CDK2 mediated phosphorylation of the retinoblastoma (Rb) family of tumor suppressor proteins during apoptosis were also observed [32]. EPI-FA-AuNPs induced apoptosis in cancer cells was evident from the reduced expression of anti-apoptotic CDK6, CDK4, and CDK2 in MCF-7 cells. In this study on the efficacy of CDK inhibition as a means to arrest the proliferation of HCC, β-actin was used as a loading control, and it showed similar expression in all the lanes. Intrinsic pathways of Western blot studies are shown in Figure 8 (B). The present study also investigated EPI-FA-AuNPs induced up-regulation of Bax proteins and down-regulation of Bcl-2 proteins in EPI-FA-AuNPs cells. p53 is a leading switch that coordinates stress signals between apoptosis and cell cycle arrest [33] is shown in Figure 8(B). EPI-FA-AuNPs induced increase in the levels of p53, the tumor suppressor protein. Caspases, a family of cysteine acid proteases, can be regarded as key factors in apoptosis [34]. In Figure 8 (B) shows that EPI-FA-AuNPs treated cells induced cleavage of caspase 3 and caspase 9. On the whole, these pH results clearly indicate that the molecular level apoptosis was induced when MCF-7 cells were treated with EPI-FA-AuNPs. Cell death was further studied based on PARP cleavage after treatment with EPI-FA-AuNPs, as seen in Figure 8 (B). Our studies showed that PARP proteins cleaved into fragments after treatment with EPI-FA-AuNPs.

High content imaging

The cellular uptake study was made in MCF-7 cell line for EPI, AuNPs, and EPI-FA-AuNPs using high content imaging methods, and the results are shown in Figure 9. EPI-FA-AuNPs' localization into the cell was compared with EPI in which bright field and fluorescent images were taken. The merged images help to calculate the localization of EPI-FA-AuNPs. Control cells without the exposure to EPI and AuNPs indicated no fluorescence [35]. The EPI-FA-AuNPs-treated cells showed maximum localization of EPI-FA-AuNPs into cells compared to EPI-treated cells.

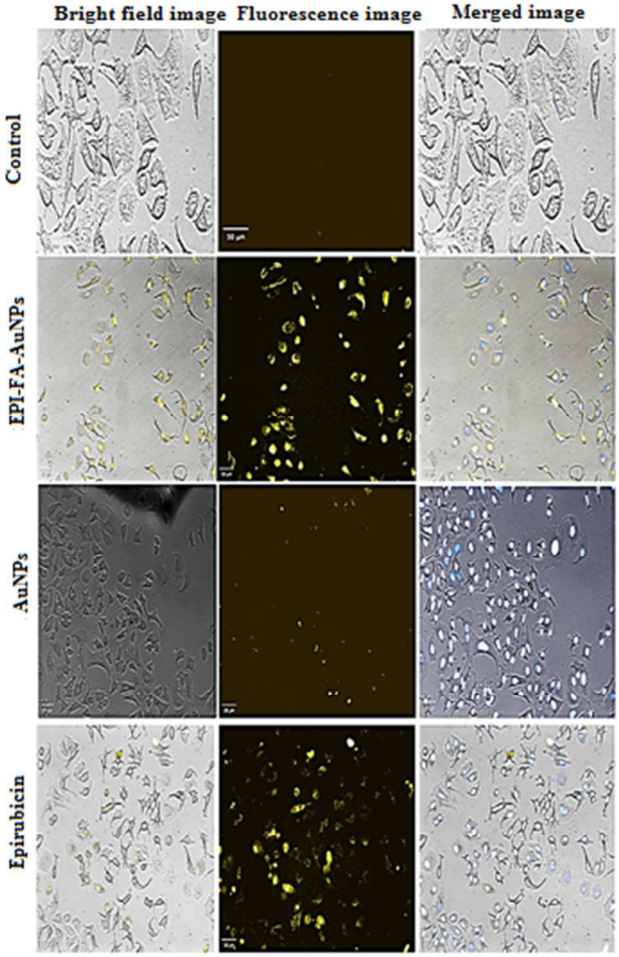

Figure 9: Drug localization studies of control, EPI, AuNPs, and EPI-FA-NPs in MCF-7 cellline.

Conclusion

To summarize the present study, a rapid and green chemistry-based method, which relies on the reduction of gold ions by *L. acidissima L* extract acting as both reducing and capping agents, has been established to synthesize AuNPs.The EPI-FA-AuNPs exhibits prominent anticancer activity against MCF-7 cells. Results of the toxicity study in the zebrafish embryo model revealed that no significant malformation occurred, ensuring that the AuNPs nanoparticles are highly compatible for drug-delivery applications. Furthermore, maximum localization into cells compared with EPI in the MCF-7 cell line was observed. The EPI-FA-AuNPs could be promising for targeting breast cancer with the enhanced therapeutic activity of EPI.

View Article Online
DOI: 10.1039/C6RA01482H

Acknowledgements

The authors are thankful to the University Grants Commission (UGC), India for financial support through the project grant no. F1-17.1/2011-12/RGNF-SC-TAM-2228/ (SA-III) to one of the authors, C. Senthil Kumar. We thank National Facility for Drug Development for Academia, Pharmaceutical and Allied Industries (NFDD) for particle size analyser facility LC-MS and FTIR studies.

References

1.B.Asadishad, M.Vossoughi, I, Alemzadeh, *Industrial & Engineering Chemistry Research* ,2010, **49**, 1958-1963.

2. W.Tian, X.Ying, J.Du, J.Guo, Y.Men, Y.Zhang, R.Li, H.Yao, J.Lou, L.Zhang, W.L Lu, *European Journal of Pharmacology,*2010, **41**, 232-243.

3. C.G. Kumar, Y.Poornachandra, S.K.Mamidyala, *Colloids and Surfaces B: Biointerfaces,* 2014,**123,** 311-317.

4. P.Joshi , S.Chakraborti , J.E. Ramirez-Vick, Z.A.Ansari, V.Shanker, P.Chakrabarti, S.P.Singh, *Colloids Surf B Biointerfaces,*2012, **95**, 195-200.

5. P.R. Devi, C.S. Kumar, P. Selvamani, N. Subramanian. K.Ruckmani, *Materials Letters,* 2015,**139**, 241-244.

6. A.K. Mittal, Y.Chisti, U.C.Banerjee, *Biotechnology Advances,*2013, **31**,346-356.

7. V.V.Makarov, A.J.Love, O.V.Sinitsyna, S.S.Makarova, I.V.Yaminsky, M.E.Taliansky, N.O.Kalinina, *Acta Naturae,*2014, **6**, 20.

8. D.T. Priyadarsini, V. Maheshu, M.Vishnupriya, S.Nishaa, J.M.Sasikumar, *Free Radicals and Antioxidants,* 2013,**3**,S62-eS69.

9.T.Betancourt, B.Brown, L. Brannon-Peppas, *Nanomedicine,*2007, **2**, 219-32.

10. K.K.Jain, *Technology in Cancer Research & Treatment*, 2005,**4** , 311-13.

11.D.C.Li, X.K.Zhong, Z.P.Zeng, *Journal of Controlled Release* ,2009,**138**,103-12.

12.Y.Lu, P.S.Low, *Advanced Drug Delivery Reviews,*2012, **64**, 342-352.

13. Z.Zhang, J.Jia, Y.Lai, Y.Ma, J.Weng, L.Sun, *Bioorganic & Medicinal Chemistry,2010,* **18** ,5528–5534.

14.M.M.Poggi, D.N.Danforth, L.C.Sciuto, S.L.Smith, S.M.Steinberg, D.J.Liewehr, C.Menard, M.E.Lippman, A.S.Lichter, R.M.Altemus, *Cancer,* 2003,**98**,697-702.

15. S.Pandey, G.Oza, A.Mewada, R.Shah, M.C.Thakur, M.Sharon, *Journal of Materials Chemistry B*, 2013, **1**,1361.

16. T.Mossman, *J Immunol Methods*, 1983,**65**,55-63.

17.S.Karthik, R.Sankar, K.Varunkumar, V.Ravikumar, *Biomedicine & Pharmacotherapy*, 2014,**68**, 327-334.

18. A.Krishnan, *The Journal of Cell Biology*,1975,**66**,188-193.

19. L.C.Tu, C.K.Chou, C.Y.Chen, Y.T.Chang, Y.C.Shen, S.F.Yeh, *Biochimica et Biophysica Acta*, 2004, **1672**, 148-156.

20. M.Ganeshkumar, M.Sathishkumar, T.Ponrasu, M.G.Dinesh, L.Sugun, *Colloids and Surfaces B: Biointerfaces*, 2013,**106**, 208-216.

21. D.Pooja, S.Panyaram, H.Kulhari, B.Reddy, S.S.Rachamalla, R.Sistla. *International Journal of Biological Macromolecules, 2015,***80**, 48-56.

22. P.Sharma, S.Sharma, V.Patial, D. Singh, Y. S. Padwad, *Clinical Queries-Nephrology*, 2014, **3**, 97-105.

23. J.A.Harris, A.G.Cheng, L.L.Cunningham, G.MacDonald, D.W.Raible, E.W.Rubel, *Journal of the Association for Research in Otolaryngology, 2003,***4**,*219*-234.

24. C.S.Kumar, M.D.Raja, D.S.Sundar, M.Gover Antoniraj, K.Ruckmani, *Carbohydrate Polymers*, 2015,**128**, 63-74.

25. E.Rafiee, S Eavani, *Materials Science and Engineering: C*, 2014, **39**, 340-343.

26. M.Tariq, M.D. Aftab Alamb, A.T. Singhc, Z.Iqbala, A. K. Pandab, S.Talegaonkara, *Colloids and Surfaces B: Biointerfaces* , 2015,**128**, 448-456.

27. D. Ormrod, K. Holm, K. Goa, C. Spencer, *Drugs Aging*, 1999,**15**, 389.

28.C.M.Halloran, P.Ghaneh, S.Shore, W.Greenhalf, L.Zumstein, D.Wilson, J.P.Neoptolemos, Costello, *European Journal of General Medicine, 2004,***6**,514-25.

29. S.Ghavami, M.Hashemi, S.R.Ande, B.Yeganeh, W.Xiao, M.Eshraghi, C.J.Bus, K.Kadkhoda, E.Wiechec, A.J.Halayko, M.Los, *Journal of Medical Genetics,2009,***46**, 497-510.

30. G.PankajRoy, Cyclin D1 and breast cancer, *The Breast* ,2006,**15**,718–727.

31. M.A.V. Velázquez, Z. Li, M. Casimiro, E.Loro, N. Homsi, R.G Pestell, *future oncology,* 2011,**7**,753-765.

32. C.G.Murphy, M.N.Dickler, *Oncologist*, 2015, **20**,483-90.

33. I.A.Hedenfalk, B.Baldetorp, A.Borg, S.M. Oredsson, *Cytometry*,1997, **29**, 321-7.

34. W.L.Sun, J.Chen, Y.P.Wang, H. Zheng, *Autophagy*, 2011, **7**, 1035-44.

35. G.Yordanov, R.Skrobanska, A.Evangelatov, *Colloids and Surfaces B: Biointerfaces*, 2012, **92**,98-105.

View Article Online
DOI: 10.1039/C6RA01482H

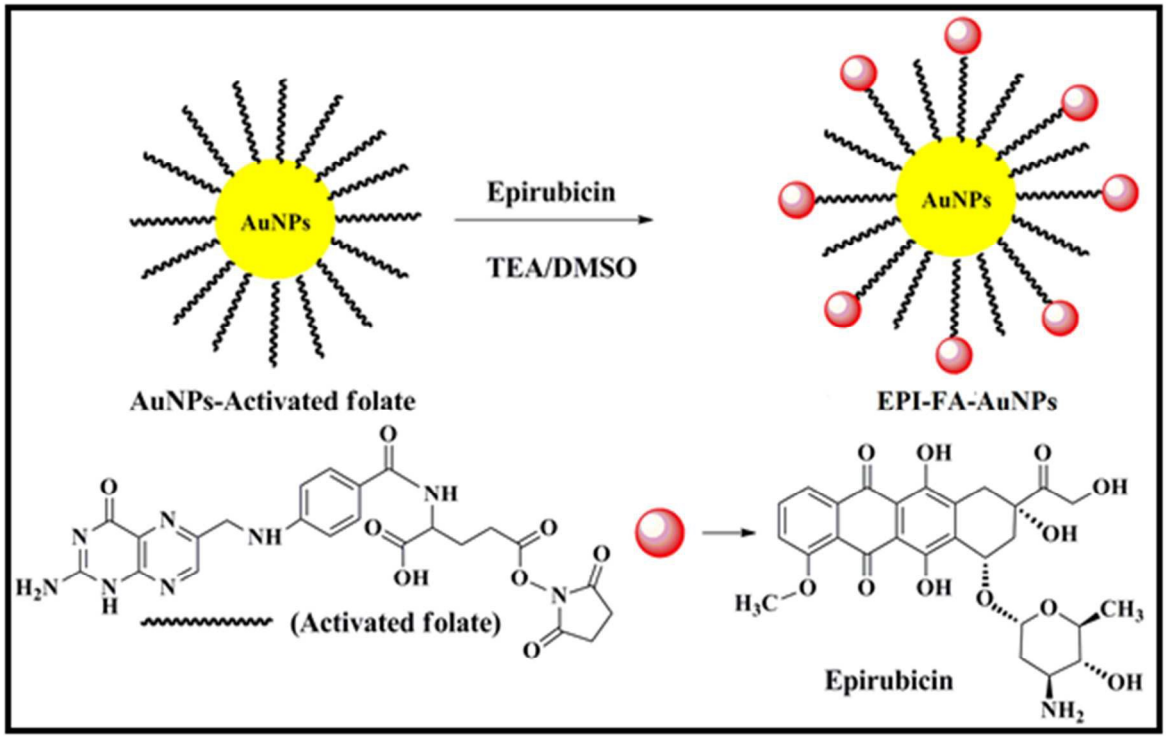

- Green synthesis of AuNPs using extract of *Limonia acidissima L* as a reducing agent
- Epirubicin was successfully loaded on Folic acid-AuNPs
- This formulation revealed better site specific delivery of epirubicin to MCF-7 cells